Supporting Information

Nested Keplerian architecture of $[Cu_{58}H_{20}(SPr)_{36}(PPh_3)_8]^{2+}$ nanocluster

Sourav Biswas,[a] Sakiat Hossian,[a] Taiga Kosaka,[a] Jin Sakai,[a] Daichi Arima,[b] Yoshiki Niihori,[a] Masaaki Mitsui,[b] De-en Jiang,[c] Saikat Das,*[a] Song Wang,*[d] and Yuichi Negishi*[a]

[a]Department of Applied Chemistry, Faculty of Science, Tokyo University of Science, Kagurazaka, Shinjuku-ku, Tokyo 162-8601, Japan. E-mail: saikatdas@rs.tus.ac.jp, negishi@rs.tus.ac.jp

[b]Department of Chemistry, College of Science, Rikkyo University, Toshima-ku, Tokyo 171-8501, Japan.

[c]Department of Chemical and Biomolecular Engineering and Department of Chemistry, Vanderbilt University, Nashville, TN 37235, USA.

[d]Hefei National Research Center for Physical Sciences at the Microscale, School of Chemistry and Materials Science, University of Science and Technology of China, Hefei, Anhui 230026, People's Republic of China. E-mail: wsong09@ustc.edu.cn

Table of contents

Experimental

Materials

Tetrakis(acetonitrile)copper(I) tetrafluoroborate $Cu(CH_3CN)_4(BF_4)$, triphenylphosphine (PPh_3), 1-propanethiol (HSPr), sodium borohydride ($NaBH_4$), sodium borodeuteride ($NaBD_4$) were procured from Sigma-Aldrich. HPLC grade solvents- chloroform, methanol, acetonitrile, and n-hexane were purchased from Tokyo Chemical Industry Co., Ltd.

Synthesis of Cu_{58} nanocluster

Initially, 50 mg (0.16 mmol) of $Cu(CH_3CN)_4BF_4$ and 50 mg (0.19 mmol) of PPh_3 were dissolved in the mixture solution of 2 mL acetonitrile and 0.5 mL chloroform at room temperature which produced a colorless solution. After 5 min of stirring, 14 μL (0.12 mmol) of HSPr was added to the reaction mixture and continued stirring. After that 50 mg (1.32 mmol) $NaBH_4$ dissolved in 2.5 mL methanol, was added into mixture drop-wise under maintain the whole temperature of the reaction at 5-10 °C and the color of the solution becomes red from colorless. The reaction was kept for another 1 hour under continuous stirring. After completion, the reaction mixture was centrifuged, and collected the red precipitate. After drying properly, the precipitate was dissolved in the solvent mixture of chloroform/hexane (volume ratio 1:1). The final clear solution was kept for crystallization at ambient conditions. After 10 days, red-colored box-shaped crystals were obtained.

Synthesis of $Cu_{58}D$ nanocluster

The same procedure was adopted whatever was mentioned for the synthesis of the Cu_{58} NC. Instead of $NaBH_4$, we have used $NaBD_4$ as a reducing agent.

X-ray Crystallography details

A single crystal was immersed in the cryoprotectant Parabar 10312 (Hampton Research, 34 Journey, Aliso Viejo, CA 92656-3317 USA) and kept at 90 K during diffraction data collection. A Bruker D8 QUEST diffractometer was used to collect the diffraction data for the single crystal using monochromated Mo Kα radiation (λ = 0.71073 Å). Although many crystals from different batches were checked for the diffraction experiment, all of them lacked higher angle

data. However, the collected diffraction data was good enough to obtain a preliminary structure containing Cu(I) ions, S, P, and a few C atoms, which was solved by SHELXT [S1] using the intrinsic phasing method in Apex3 Bruker Software Suite.[S2] Later, during refinement the full crystal structure was completed using the full-matrix least squares method against F^2 by SHELXL-2018/3 in Olex2 GUI[S3] All the atoms including propylthiolates, *n*-heaxane solvent, and one $[BF_4]^-$ anion were refined anisotropically. We faced challenges modelling the second $[BF_4]^-$ anion, which is situated on a complex special symmetry position where corresponding q peaks are located on both 3-fold and 6-fold special symmetry positions. However, we have deliberately left the electron q-peaks unmasked to provide readers a clearer understanding of the total structure (even though cif file will not directly show q peaks). A few disordered phenyl rings were fixed by AFIX 66. Although Cu_{58} NC has twenty hydrides (H^-), which were confirmed by ESI-MS and theoretical calculations, they could not be assigned and refined stably.

Although few check cif alerts are there, we have provided a comprehensive response as follows

 # start Validation Reply Form

_vrf_THETM01_Cu58
;
PROBLEM: The value of sine(theta_max)/wavelength is less than 0.550.
RESPONSE: Despite our persistent efforts, we were unable to obtain a new data set with a higher resolution than 1.2 Å. This limitation can be attributed to the inherent weak diffracting ability of the Cu_{58} cluster.
;
_vrf_DIFMX02_Cu58
;
PROBLEM: The maximum difference density is > 0.1*ZMAX*0.75.
RESPONSE: The highest electron density, measuring 2.92, corresponds to the disordered second $[BF_4]^-$ anion. Due to its placement in a complex special symmetry position involving both 3-fold and 6-fold symmetry positions, we encountered difficulties in accurately modeling this component. As a result, it remains unresolved in the structure.
;
_vrf_PLAT029_Cu58
;
PROBLEM: _diffrn_measured_fraction_theta_full value Low . 0.919 Why?
RESPONSE: During the initial data collection, the unit cell and space group exhibited higher symmetry, specifically cubic symmetry, compared to the final space group and symmetry in which the data was ultimately solved and refined. Consequently, the completeness of the data was less than 100% due to this change.
Regrettably, despite our extensive efforts spanning over six months, both before the first communication and during the review stage, we could not achieve a resolution improvement beyond 1.20 Å for any of the subsequent data sets. Therefore, the only enhancement we could make was in the completeness of the initial data set, which increased from 89% to 92% by incorporating all the reflection frames.
;
_vrf_PLAT307_Cu58
;
PROBLEM: Isolated Metal Atom found in Structure (Unusual) Cu02 Check.
RESPONSE: Each of these copper ion (Cu02, Cu04) in our structure forms bonds with four hydride atoms. However, these hydrides were not assigned and refined crystallographically. Therefore, these alerts are generated by those isolated Cu ions. Nonetheless, we were able to predict their presence using ESI-MS (Electrospray Ionization Mass Spectrometry) and locate them through DFT (Density Functional Theory) calculations. The combination of experimental and computational methods allowed us to confirm the existence of the hydride atoms associated with those copper ions. Therefore, they are not isolated.

;
_vrf_PLAT097_Cu58
;
PROBLEM: Large Reported Max. (Positive) Residual Density 2.93 eA-3.
RESPONSE: We believe that the highest electron density, measuring 2.92, corresponds to the disordered second [BF4]- anion. Unfortunately, this anion could not be accurately modeled due to its presence in both a 3-fold and 6-fold special symmetry position. As a result, the precise structural representation of this component remains unresolved.
;
_vrf_PLAT341_Cu58
;
PROBLEM: Low Bond Precision on C-C Bonds ..... 0.03056 Ang.
RESPONSE: The structure consists of a notable presence of 36 carbon chains, specifically propyl thiolates. These chains inherently exhibit higher thermal parameters and disorder, which consequently lower the precision of the C-C bonds within them. It is important to acknowledge this characteristic when considering the structural analysis of the propyl thiolate chains.
;
_vrf_PLAT601_Cu58
;
PROBLEM: Unit Cell Contains Solvent Accessible VOIDS of . 104 Ang**3.
RESPONSE: We believe that this particular region of the structure comprises a disordered second $[BF_4]^-$ ion. Unfortunately, this ion could not be accurately modeled due to its challenging placement on a complex special symmetry position involving both 3-fold and 6-fold symmetry elements. As a result, the precise modeling of this ion within the structure was not possible. However, we did not mask to show readers that Cu58 cluster, indeed, has two $[BF_4]^-$ anions.
;
_vrf_DIFMX02_ALERT_1_C
;
PROBLEM: The maximum difference density is > 0.1*ZMAX*0.75 The relevant atom site should be identified.
RESPONSE: The highest electron density, measuring 2.92, corresponds to the disordered second [BF4]- anion. As it is located in a complex special symmetry position involving both 3-fold and 6-fold symmetry positions, we encountered difficulties in accurately modeling this component. As a result, it remains unresolved in the structure.
;
_vrf_PLAT041_ALERT_1_C
;
PROBLEM: Calc. and Reported SumFormula Strings Differ Please Check.
RESPONSE: [BF4]- anion has a 3 fold symmetry whereas Cu58 cluster has a 6 fold symmetry, as a result, asymmetric unit of the crystal contains 1/6 of the Cu58 cluster and 1/3 of [BF4]- anion. Therefore, when SumFormula is calculated, it shows one additional [BF4]- anion.
;
_vrf_PLAT042_ALERT_1_C
;
PROBLEM: Calc. and Reported MoietyFormula Strings Differ Please Check.
RESPONSE: [BF4]- anion has a 3 fold symmetry whereas Cu58 cluster has a 6 fold symmetry, as a result, asymmetric unit of the crystal contains 1/6 of the Cu58 cluster and 1/3 of [BF4]- anion. Therefore, when MoietyFormula i calculated, it shows one additional [BF4]- anion.
;
_vrf_PLAT043_ALERT_1_C
;
PROBLEM: Calculated and Reported Mol. Weight Differ by .. 86.74 Check.
RESPONSE: [BF4]- anion has a 3 fold symmetry whereas Cu58 cluster has a 6 fold symmetry, as a result, asymmetric unit of the crystal contains 1/6 of the Cu58 cluster and 1/3 of [BF4]- anion. Therefore, when Mol. Weight is calculated, it shows one additional [BF4]- anion.
;
_vrf_PLAT094_ALERT_2_C
PROBLEM: Ratio of Maximum / Minimum Residual Density .... 2.31 Report.
RESPONSE: An electron density peak measuring 2.92 has intentionally been left unassigned to illustrate the presence of the unresolved disordered second [BF4]- ion. Consequently, this decision contributes to a higher ratio of residual density within the structure. The purpose of highlighting this unassigned peak is to convey the existence of the disordered [BF4]- anion could not be modeled.
;
_vrf_PLAT220_ALERT_2_C
;
PROBLEM: NonSolvent Resd 1 C Ueq(max)/Ueq(min) Range 3.8 Ratio.
RESPONSE: This is part of carbon chain of propyl thiolates or hexane solvent of the crystal. PLAT222_ALERT_3_C NonSolvent Resd 1 H Uiso(max)/Uiso(min) Range 4.7 Ratio Author Response: Presence of high thermal carbon atoms making the attached -H with higher Uiso(max)/Uiso(min)range.
;
_vrf_PLAT241_ALERT_2_C
;
PROBLEM: High 'MainMol' Ueq as Compared to Neighbors of C35 Check.

```
RESPONSE: C35 is a part of phenyl ring of a PPh3 ligand, and this carbon atom is bonded to C25
which is directly bonded to P of PPh3 ligand and has normal thermal parameters. As a result,
C35 exhibits higher relative thermal parameters compared to its neighboring carbon atoms.
;
PLAT242_ALERT_2_C
;
PROBLEM: Low 'MainMol' Ueq as Compared to Neighbors of C13 Check.
RESPONSE: C13 is the middle carbon of a propylthiolate ligand, and this carbon is bonded with
terminal carbon C37 of same propylthiolate ligand which has higher thermal parameter. This is
the reason this alert was generated.
;
_vrf_PLAT242_ALERT_2_C
;
PROBLEM: Low 'MainMol' Ueq as Compared to Neighbors of C26 Check.
RESPONSE: C13 is the middle carbon of a propylthiolate ligand, and this carbon is bonded with
terminal carbon C37 of same propylthiolate ligand which has higher thermal parameter. This is
the reason this alert was generated.
;
_vrf_PLAT250_ALERT_2_C
;
PROBLEM: Large U3/U1 Ratio for Average U(i,j) Tensor .... 2.6 Note.
RESPONSE: Few atoms of chain like propyl thiolates and a n-hexane solvent have higher thermal
parameters.
;
_vrf_PLAT260_ALERT_2_C
;
PROBLEM: Large Average Ueq of Residue Including F1 0.261 Check.
RESPONSE: It is part of the [BF4]- anion with higher thermal parameters.
;
_vrf_PLAT413_ALERT_2_C
;
PROBLEM: Short Inter XH3 .. XHn H33 ..H41C . 2.01 Ang. -2/3+y,2/3-x+y,5/3-z = 17_456 Check.
RESPONSE: Attached carbon atom of a propylthiolate chain has higher thermal parameters, as a
result, refinement of the H, especially direction, may be not perfect, consequently, two H atoms
of two different cluster come closer.
;
# end Validation Reply Form
```

Computational details

A deep-learning model[S4] was used to predict hydride sites in copper cluster. This convolutional neural network takes the heavy-atom coordinates of the cluster obtained from the single-crystal X-ray diffraction as input and predicts the occupancy for each potential hydride site in the cluster. The details of the Cu-H neural network can be found in previous studies.[S4,S5] In this work, the X-ray structures of $[Cu_{58}H_{20}(SCH_2CH_2CH_3)_{36}(PPh_3)_8]^{2+}$ (i.e., the coordinates of Cu, C, P, and S in the cluster) were used as input. The model predicted that there are 20 highly probable hydride sites, which are consistent with the hydride number obtained from the experimental measurements. To validate the prediction, DFT calculation was performed by using the Vienna ab initio simulation package (VASP) software. The Perdew–Burke–Ernzerhof (PBE) form of the generalized-gradient approximation (GGA) was used for electron exchange and correlation.[S6] The projector-augmented-wave (PAW) method[S7] was used to describe the electron-core interaction with the cutoff energy of 450 eV for the planewave bases.

Instrumentation

UV-Vis absorption spectra were obtained with a JASCO V-670 UV-VIS-NIR spectrophotometer. Fluorescence measurements were conducted at room temperature with a linearly polarized continuous wave (cw) 405MDLC (SUNSHINE) diode laser as an excitation source and the spectra was recorded using a SpectraPro 2300i polychromator coupled with a liquid-nitrogen-cooled charge coupled device camera (Spec-10:100B/LN, Roper Scientific). The lifetime of the emission was measured by synchronize of laser and avalanche photodiode (APD, SPCM-AQRH-61, Perkin-Elmer), which were fed to the time-correlated single photon counting (TC-SPC) card (TimeHarp 260, PicoQuant) operating in time-tagged and time-resolved modes. Recording and analysis of data were performed using the SymPhoTime 64 (PicoQuant) software. The Fluorolog-3 spectrofluorimeter was utilized to establish the relative quantum yield. This determination involved finding the optimal excitation wavelength, which closely matched with $[Ru(bipyridine)_3]Cl_2$. The concentration of the solutions was standardized by adjusting the absorption to 0.05 OD, and the quantum yield measurement was conducted under room temperature condition. Scanning electron microscopy (SEM) images were recorded using JEOL JSM-7000FSHL field emission scanning electron microscope. Electrospray ionization mass spectrometry was performed using a reflectron-type time of flight MS system (Bruker, microTOF II). The NCs were dissolved in a mixture of chloroform and acetonitrile. The isotope distribution was calculated using an isotope pattern simulator (JEOL, Isotope Pattern Simulator).

Table S1. Crystal data and structure refinement parameters.

Table 1 Crystal data and structure refinement for Cu_{58}.	
Identification code	Cu_{58}
Empirical formula	$C_{270}H_{414}BCu_{58}F_4P_8S_{36}$
CCDC no	2255364
Formula weight	8834.71
Temperature/K	90.15
Crystal system	trigonal
Space group	R-3
a/Å	23.3990(7)
b/Å	23.3990(7)
c/Å	57.171(4)
α/°	90
β/°	90
γ/°	120
Volume/Å^3	27108(3)
Z	3
ρcalcg/cm^3	1.639
μ/mm 1	3.615
F(000)	13482.0
Crystal size/mm^3	0.6 × 0.6 × 0.4
Radiation	MoKα (λ = 0.71073)
2Θ range for data collection/°	4.082 to 41.62
Index ranges	$-20 \leq h \leq 23$, $-23 \leq k \leq 23$, $-31 \leq l \leq 55$
Reflections collected	14513
Independent reflections	5187 [R_{int} = 0.0539, R_{sigma} = 0.0830]
Data/restraints/parameters	5817/485/609
Goodness-of-fit on F^2	1.064
Final R indexes [I>=2σ (I)]	R_1 = 0.0587, wR_2 = 0.1671
Final R indexes [all data]	R_1 = 0.1114, wR_2 = 0.2027
Largest diff. peak/hole / e Å^{-3}	2.93/-1.27

Additional Information on Crystal Analysis:

Details:

1. Fixed Uiso

At 1.2 times of:

All C (H) groups, All C (H, H) groups

At 1.5 times of:

All C (H, H, H) groups

2. Restrained distances

F1-B1 = F2-B1

1.43 with sigma of 0.02

C25-C17

1.39 with sigma of 0.02

C16-C15 = C41-C15

1.53 with sigma of 0.02

3. Uiso/Uaniso restraints and constraints

C1 ≈ C15 ≈ C48 ≈ C4 ≈ C9 ≈ C6 ≈ C27 ≈ C8 ≈ C2

≈ C10 ≈ C12 ≈ C25 ≈ C14 ≈ C16 ≈ C18 ≈ C17 ≈ C20

≈ C19 ≈ C22 ≈ C41 ≈ C24 ≈ C3 ≈ C26 ≈ C13 ≈ C28

≈ C7 ≈ C30 ≈ C29 ≈ C32 ≈ C31 ≈ C34 ≈ C33 ≈ C36

≈ C35 ≈ C38 ≈ C37 ≈ C40 ≈ C39 ≈ C42 ≈ C5 ≈ C44

≈ C46: within 1.7A with sigma of 0.04 and sigma for terminal atoms of 0.08

within 1.7A

C21 ≈ C43 ≈ C11 ≈ C45 ≈ C47 ≈ C23: within 1.7A with sigma

of 0.02 and sigma for terminal atoms of 0.04 within 1.7A

4. Rigid body (RIGU) restrains

C1, C15, C48, C4, C9, C6, C27, C8, C2, C10, C12, C25, C14, C16, C18, C17, C20,

C19, C22, C41, C24, C3, C26, C13, C28, C7, C30, C29, C32, C31, C34, C33, C36,

C35, C38, C37, C40, C39, C42, C5, C44, C46

with sigma for 1-2 distances of 0.004 and sigma for 1-3 distances of 0.004

C21, C43, C11, C45, C23, C47

with sigma for 1-2 distances of 0.004 and sigma for 1-3 distances of 0.004

F1, F2, B1

with sigma for 1-2 distances of 0.004 and sigma for 1-3 distances of 0.004

5. Others

Fixed Sof: C21(0.5) H21A(0.5) H21B(0.5) H21C(0.5) C43(0.5) H43A(0.5)

H43B(0.5) C11(0.5) H11A(0.5) H11B(0.5) C45(0.5) H45A(0.5) H45B(0.5) C23(0.5)

H23A(0.5) H23B(0.5) H23C(0.5) C47(0.5) H47A(0.5) H47B(0.5)

6.a Secondary CH_2 refined with riding coordinates:

C1(H1A,H1B), C6(H6A,H6B), C8(H8A,H8B), C12(H12A,H12B), C14(H14A,H14B),

C16(H16A,H16B), C24(H24A,H24B), C26(H26A,H26B), C36(H36A,H36B),

C13(H13A,H13B), C7(H7A,H7B), C15(H15A,H15B), C43(H43A,H43B),

C11(H11A,H11B), C45(H45A,H45B), C47(H47A,H47B)

6.b Aromatic/amide H refined with riding coordinates:

C4(H4), C10(H10), C20(H20), C22(H22), C30(H30), C32(H32), C34(H34), C38(H38),

C42(H42), C48(H48), C3(H3), C27(H27), C29(H29), C31(H31), C33(H33), C17(H17), C35(H35), C9(H9), C19(H19), C39(H39)

6.c Idealised Me refined as rotating group:

C44(H44A,H44B,H44C), C46(H46A,H46B,H46C), C2(H2A,H2B,H2C), C37(H37A,H37B, H37C), C5(H5A,H5B,H5C), C41(H41A,H41B,H41C), C21(H21A,H21B,H21C), C23(H23A,H23B,H23C)

Table S2. Average bond lengths between Cu-Cu

Bond lengths (Å)			Average bond lengths (Å)
Cu4	$Cu4^{2}$	2.658(3)	2.654±0.004
Cu4	$Cu4^{1}$	2.658(3)	
Cu4	Cu8	2.650(3)	
Cu4	$Cu7^{3}$	2.758(2)	2.748 ±0.009
Cu4	Cu7	2.751(2)	
Cu4	$Cu7^{1}$	2.737(3)	
Cu8	Cu7	2.7552(16)	
Cu8	$Cu7^{4}$	2.7550(16)	
Cu8	$Cu3^{4}$	2.690(4)	2.703 ±0.017
Cu8	$Cu3^{3}$	2.690(4)	
Cu8	Cu3	2.690(4)	
Cu4	$Cu9^{3}$	2.732(3)	
Cu4	$Cu5^{1}$	2.688(2)	
Cu4	Cu11	2.702(2)	
Cu7	Cu9	2.791(2)	2.771±0.030
Cu7	Cu5	2.719(3)	
Cu11	Cu7	2.783(2)	
Cu3	Cu7	2.719(3)	
Cu1	Cu11	2.740(3)	2.748±0.024
Cu1	Cu5	2.787(2)	
Cu6	Cu3	2.747(2)	
Cu6	Cu9	2.720(3)	

Table S3. Other bond length details

S6	C8	1.853(16)	C12	C13	1.51(2)
S3	C12	1.825(16)	C14	C26	1.51(2)
Cu1	S1[1]	2.338(4)	S2	C16	1.856(16)
Cu1	S4	2.223(4)	S5	C1	1.845(14)
Cu1	S6	2.225(5)	P1	C18	1.81(2)
P1	C28	1.817(15)	C16	C15	1.541(18)
P1	C40	1.838(17)	C24	C44	1.49(3)
P2	C25[3]	1.82(2)	C26	C2	1.54(3)
P2	C25[4]	1.82(2)	C28	C48	1.39(3)
P2	C25	1.82(2)	C30	C27	1.35(3)
C1	C7	1.50(3)	C36	C46	1.53(2)
C4	C10	1.40(2)	C38	C42	1.37(3)
C4	C40	1.40(2)	C13	C37	1.49(2)
C6	C36	1.533(19)	C7	C5	1.53(3)
C8	C24	1.486(18)	C31	C9	1.39(3)
C10	C38	1.32(2)	C33	C19	1.39(4)
Cu6	S3[4]	2.345(4)	C33	C39	1.38(4)
Cu6	S2	2.225(4)	C17	C19	1.41(3)
Cu6	S5	2.227(5)	C35	C39	1.43(3)
C18	C34	1.34(3)	C21	C11	1.64(5)
C18	C3	1.43(2)	C43	C45	1.49(6)
C20	C40	1.365(19)	C20	C42	1.42(3)
C22	C28	1.41(2)	C22	C30	1.40(2)
Cu10	S6[2]	2.378(4)	Cu10	S4	2.398(5)
Cu10	P1	2.239(4)	Cu10	S2[1]	2.385(4)
C32	C48	1.38(2)	C32	C27	1.40(3)
C34	C29	1.44(3)	Cu11	S6	2.266(3)

Cu11	S3	2.265(5)	C3	C31	1.36(3)
C25	C17	1.405(18)	C25	C35	1.40(3)
Cu3	S3	2.275(4)	Cu3	S5	2.253(5)
C29	C9	1.42(3)	C15	C41	1.496(17)
Cu7	S1	2.438(4)	Cu7	S3	2.441(5)
Cu2	$S5^{3}$	2.368(4)	Cu2	S5	2.368(4)
Cu2	$S5^{4}$	2.368(4)	Cu2	P2	2.237(11)
C43	C11	1.41(4)	S4	C6	1.844(15)
Cu9	S1	2.263(4)	F2	B1	1.43(2)
Cu9	S2	2.264(5)	C45	C47	1.57(6)
Cu5	S1	2.276(4)	C23	C47	1.66(6)
Cu5	S4	2.251(4)	F1	B1	1.395(16)
S1	C14	1.846(16)			

Table S4. Probability chart of hydride occupancy from CNN.

Site Rank	Probability of H^- occupancy from CNN	$Cu_{58}H_{20}$	Site Rank	Probability of H^- occupancy from CNN	$Cu_{58}H_{20}$
1	99.95%	Yes	12	99.26%	Yes
2	99.90%	Yes	13	99.15%	Yes
3	99.81%	Yes	14	99.09%	Yes
4	99.74%	Yes	15	98.54%	Yes
5	99.71%	Yes	16	97.76%	Yes
6	99.71%	Yes	17	97.51%	Yes
7	99.60%	Yes	18	97.46%	Yes
8	99.55%	Yes	19	96.13%	No
9	99.51%	Yes	20	95.68%	Yes
10	99.33%	Yes	21	93.03%	Yes
11	99.30%	Yes	site 19 is the center of cluster core		

Table S5. Bader charge distribution

Index	element	x_frac	y_frac	z_frac	x	y	z	Bader charge
Cu1	Cu	0.43216	0.34617	0.57215	11.02008	8.827335	14.58983	0.384324
Cu2	Cu	0.35222	0.32116	0.51138	8.98161	8.18958	13.04019	0.384792
Cu3	Cu	0.67881	0.349	0.52088	17.30966	8.8995	13.28244	0.389532
Cu4	Cu	0.31554	0.66498	0.65475	8.04627	16.95699	16.69613	0.405158
Cu5	Cu	0.32787	0.6394	0.31802	8.360685	16.3047	8.10951	0.412294
Cu6	Cu	0.44864	0.54288	0.44575	11.44032	13.84344	11.36663	0.254576
Cu7	Cu	0.45722	0.4399	0.4535	11.65911	11.21745	11.56425	0.246992
Cu8	Cu	0.51417	0.37264	0.51267	13.11134	9.50232	13.07309	0.329116
Cu9	Cu	0.35972	0.4184	0.42239	9.17286	10.6692	10.77095	0.387633
Cu10	Cu	0.34989	0.54051	0.41338	8.922195	13.78301	10.54119	0.388331
Cu11	Cu	0.56035	0.44899	0.4564	14.28893	11.44925	11.6382	0.245529
Cu12	Cu	0.5567	0.45637	0.55966	14.19585	11.63744	14.27133	0.26304
Cu13	Cu	0.35375	0.42889	0.58388	9.020625	10.9367	14.88894	0.385153
Cu14	Cu	0.33249	0.49715	0.661	8.478495	12.67733	16.8555	0.386211
Cu15	Cu	0.5935	0.35974	0.58148	15.13425	9.17337	14.82774	0.387065
Cu16	Cu	0.34399	0.472	0.33504	8.771745	12.036	8.54352	0.384108
Cu17	Cu	0.34323	0.32974	0.67905	8.752365	8.40837	17.31578	0.410219
Cu18	Cu	0.37547	0.48833	0.49965	9.574485	12.45242	12.74108	0.325132
Cu19	Cu	0.43688	0.33771	0.45301	11.14044	8.611605	11.55176	0.384985
Cu20	Cu	0.67907	0.35868	0.68899	17.31629	9.14634	17.56925	0.415267
Cu21	Cu	0.59836	0.35083	0.4523	15.25818	8.946165	11.53365	0.386029
Cu22	Cu	0.34323	0.55593	0.57427	8.752365	14.17622	14.64389	0.386978
Cu23	Cu	0.6619	0.44726	0.43067	16.87845	11.40513	10.98209	0.384689
Cu24	Cu	0.67342	0.5018	0.34317	17.17221	12.7959	8.750835	0.381934
Cu25	Cu	0.66268	0.52567	0.66982	16.89834	13.40459	17.08041	0.3936

Cu26	Cu	0.35513	0.30352	0.34358	9.055815	7.73976	8.76129	0.412753
Cu27	Cu	0.55184	0.55215	0.44843	14.07192	14.07983	11.43497	0.262423
Cu28	Cu	0.63016	0.51071	0.50715	16.06908	13.02311	12.93233	0.322479
Cu29	Cu	0.56387	0.57462	0.34688	14.37869	14.65281	8.84544	0.385583
Cu30	Cu	0.44119	0.56365	0.34408	11.25035	14.37308	8.77404	0.384351
Cu31	Cu	0.54825	0.5595	0.55169	13.98038	14.26725	14.0681	0.259561
Cu32	Cu	0.57795	0.4137	0.35944	14.73773	10.54935	9.16572	0.385475
Cu33	Cu	0.52276	0.32501	0.35041	13.33038	8.287755	8.935455	0.385707
Cu34	Cu	0.65741	0.45423	0.59276	16.76396	11.58287	15.11538	0.390406
Cu35	Cu	0.49632	0.65037	0.32538	12.65616	16.58444	8.29719	0.38666
Cu36	Cu	0.69146	0.33478	0.35244	17.63223	8.53689	8.98722	0.406525
Cu37	Cu	0.50764	0.48998	0.37557	12.94482	12.49449	9.577035	0.322858
Cu38	Cu	0.65175	0.56622	0.42189	16.61963	14.43861	10.7582	0.381362
Cu39	Cu	0.64618	0.58272	0.5832	16.47759	14.85936	14.8716	0.384761
Cu40	Cu	0.4518	0.40272	0.35583	11.5209	10.26936	9.073665	0.384407
Cu41	Cu	0.55114	0.59632	0.64954	14.05407	15.20616	16.56327	0.384349
Cu42	Cu	0.4838	0.67512	0.65531	12.3369	17.21556	16.71041	0.386107
Cu43	Cu	0.51144	0.34978	0.68049	13.04172	8.91939	17.3525	0.385974
Cu44	Cu	0.66384	0.66919	0.32621	16.92792	17.06435	8.318355	0.413268
Cu45	Cu	0.44479	0.55044	0.54892	11.34215	14.03622	13.99746	0.253106
Cu46	Cu	0.49868	0.50831	0.63021	12.71634	12.96191	16.07036	0.329863
Cu47	Cu	0.40664	0.64804	0.55135	10.36932	16.52502	14.05943	0.387665
Cu48	Cu	0.41157	0.63858	0.42874	10.49504	16.28379	10.93287	0.380183
Cu49	Cu	0.45332	0.44749	0.55694	11.55966	11.411	14.20197	0.2614
Cu50	Cu	0.56806	0.66209	0.55633	14.48553	16.8833	14.18642	0.387488
Cu51	Cu	0.65134	0.67815	0.49432	16.60917	17.29283	12.60516	0.387488
Cu52	Cu	0.56828	0.43578	0.66258	14.49114	11.11239	16.89579	0.385125
Cu53	Cu	0.32578	0.65006	0.48676	8.30739	16.5765	12.4123	0.383694

						3	8	
Cu54	Cu	0.6503	0.69424	0.66256	16.5826 5	17.7031 2	16.8952 8	0.414533
Cu55	Cu	0.49234	0.6266	0.49333	12.5546 7	15.9783	12.5799 2	0.327123
Cu56	Cu	0.4312	0.58581	0.64609	10.9956	14.9381 6	16.4753	0.382442
Cu57	Cu	0.44079	0.42452	0.6588	11.2401 5	10.8252 6	16.7994	0.386733
Cu58	Cu	0.57255	0.65324	0.42927	14.6000 3	16.6576 2	10.9463 9	0.385329
H373	H	0.5719	0.40514	0.51205	14.5834 5	10.3310 7	13.0572 8	-0.272176
H374	H	0.59079	0.59245	0.40652	15.0651 5	15.1074 8	10.3662 6	-0.32226
H375	H	0.51148	0.43094	0.4058	13.0427 4	10.9889 7	10.3479	-0.269665
H376	H	0.58338	0.6058	0.5907	14.8761 9	15.4479	15.0628 5	-0.327951
H377	H	0.59909	0.42277	0.60415	15.2768	10.7806 4	15.4058 3	-0.331057
H378	H	0.40031	0.58996	0.58569	10.2079 1	15.0439 8	14.9351	-0.32971
H379	H	0.40155	0.48648	0.43806	10.2395 3	12.4052 4	11.1705 3	-0.275428
H380	H	0.41559	0.40618	0.59903	10.5975 5	10.3575 9	15.2752 7	-0.331851
H381	H	0.42215	0.39274	0.41572	10.7648 3	10.0148 7	10.6008 6	-0.328285
H382	H	0.39916	0.49531	0.56127	10.1785 8	12.6304 1	14.3123 9	-0.274799
H383	H	0.55548	0.60633	0.49693	14.1647 4	15.4614 2	12.6717 2	-0.284649
H384	H	0.49394	0.56908	0.60209	12.5954 7	14.5115 4	15.3533	-0.275858
H385	H	0.43231	0.59739	0.49268	11.0239 1	15.2334 5	12.5633 4	-0.276609
H386	H	0.60941	0.5044	0.44342	15.5399 6	12.8622	11.3072 1	-0.272049
H387	H	0.60077	0.51272	0.56648	15.3196 4	13.0743 6	14.4452 4	-0.273154
H388	H	0.60617	0.4098	0.4208	15.4573 4	10.4499	10.7304	-0.328892
H389	H	0.5009	0.55358	0.39459	12.7729 5	14.1162 9	10.0620 5	-0.280963
H390	H	0.40648	0.57648	0.40121	10.3652 4	14.7002 4	10.2308 6	-0.324055
H391	H	0.44923	0.39002	0.50904	11.4553 7	9.94551	12.9805 2	-0.274855
H392	H	0.50424	0.44602	0.60813	12.8581 2	11.3735 1	15.5073 2	-0.272913

Table S6. Parameters obtained from TCSPC measurement

Component	**τ (ns)**	***A***	***f***
1	5855	0.007	0.715
2	8.90	0.98	0.147
3	596	0.013	0.137

Fitting parameter χ^2 is 1.12, τ is the lifetime of each individual component, A is the amplitude and f determine the fractional population of each component.

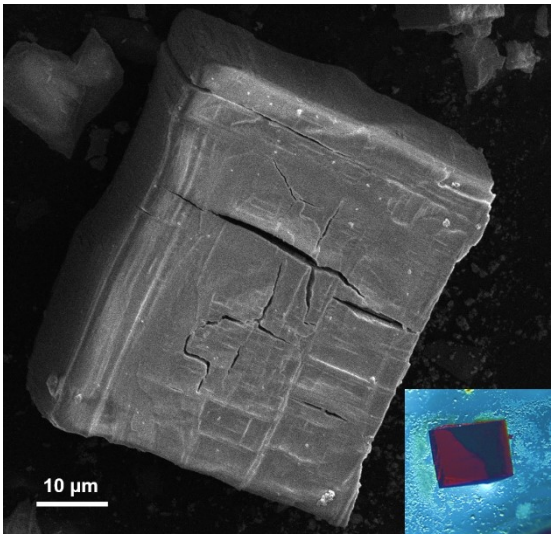

Fig. S1 SEM and optical microscope image of Cu_{58} NC crystal.

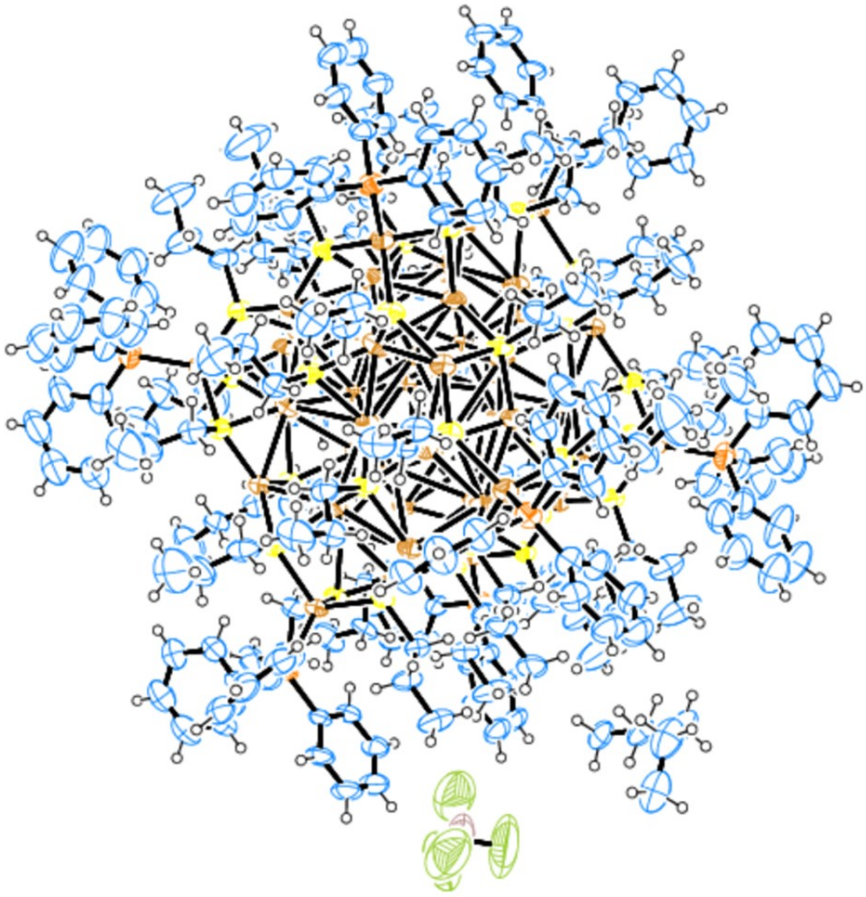

Fig. S2 Thermal ellipsoid (50%) of all atoms present in Cu_{58} NC.

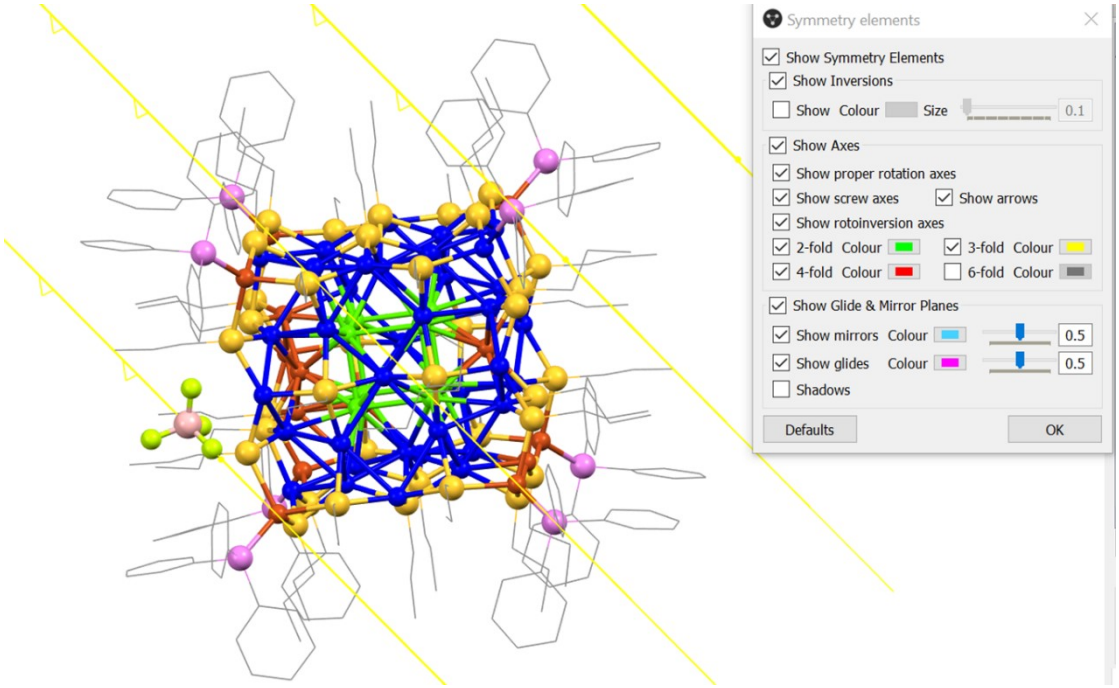

Fig. S2 Symmetry elements of Cu_{58} NC. Color legend: Cu, light green, blue and brown; S, yellow; P, violet; B, pink; F, yellowish-green; C, grey stick; H atoms are omitted.

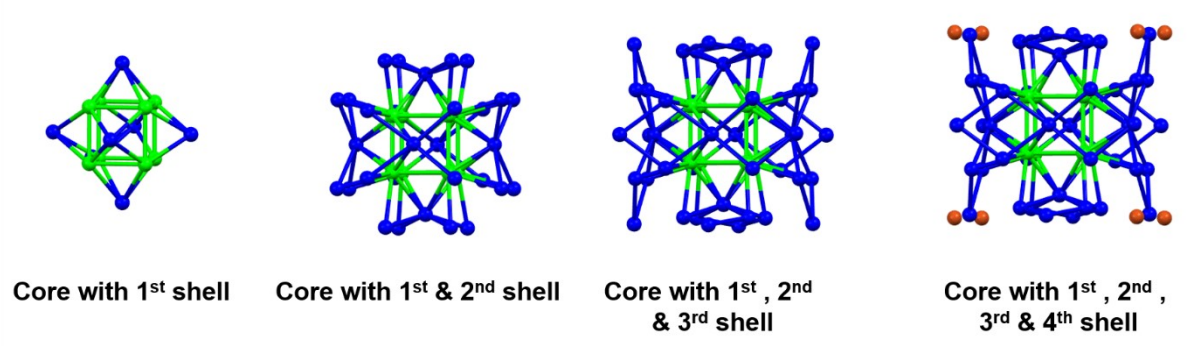

Fig. S4 Connections and among the layers of Cu atoms and their positions in Cu_{58} NC. Color legend: Cu, light green, blue and brown.

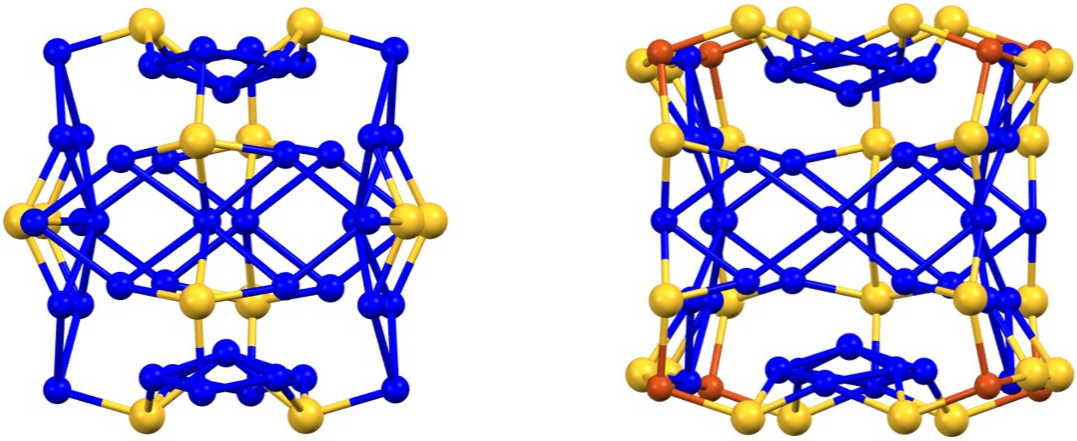

Fig. S5 Bridging among the shell layers in Cu_{58} NC. Color legend: Cu, blue and brown; S, yellow.

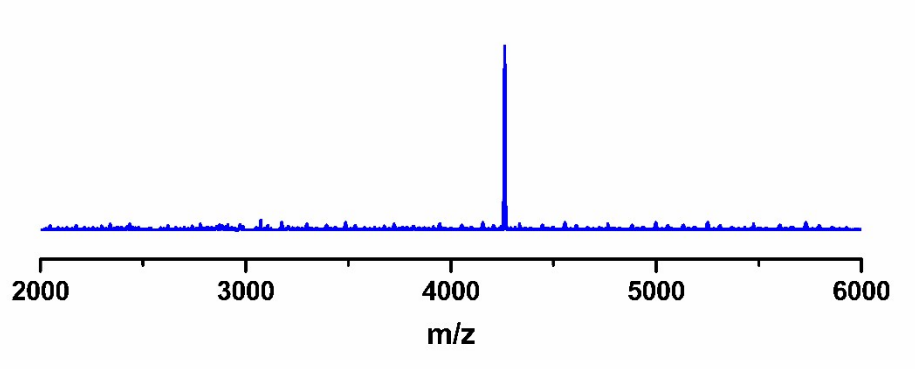

Fig. S6 ESI mass spectrum of $Cu_{58}D$ nanocluster.

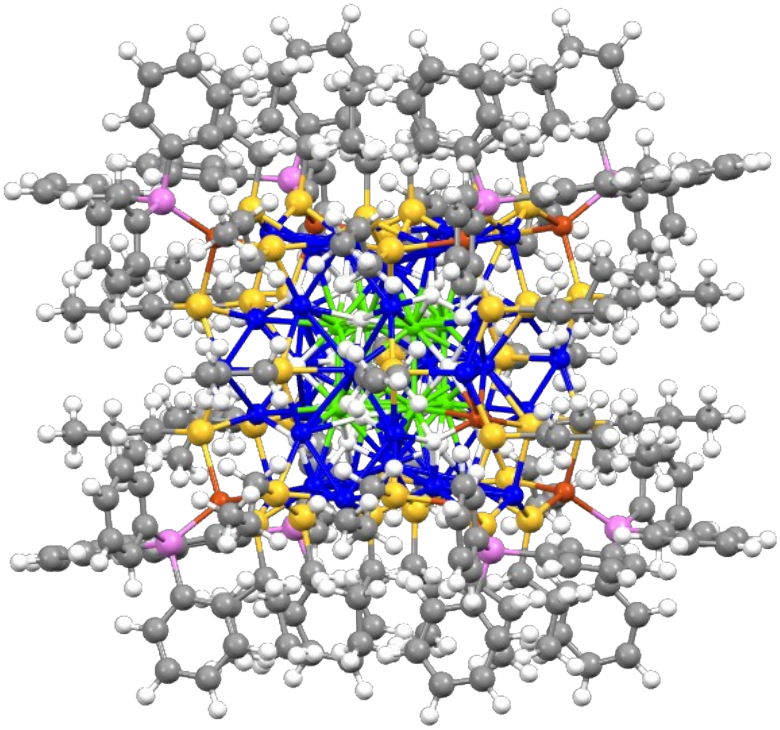

Fig. S7 DFT-optimized structure of the Cu_{58} NC after placing the 20 hydrides into the X-ray structure (the sites to place hydrides were predicted from machine learning; see Fig. S8). Color legend: Cu, light green, blue and brown; S, yellow; P, violet; C, grey; H, white.

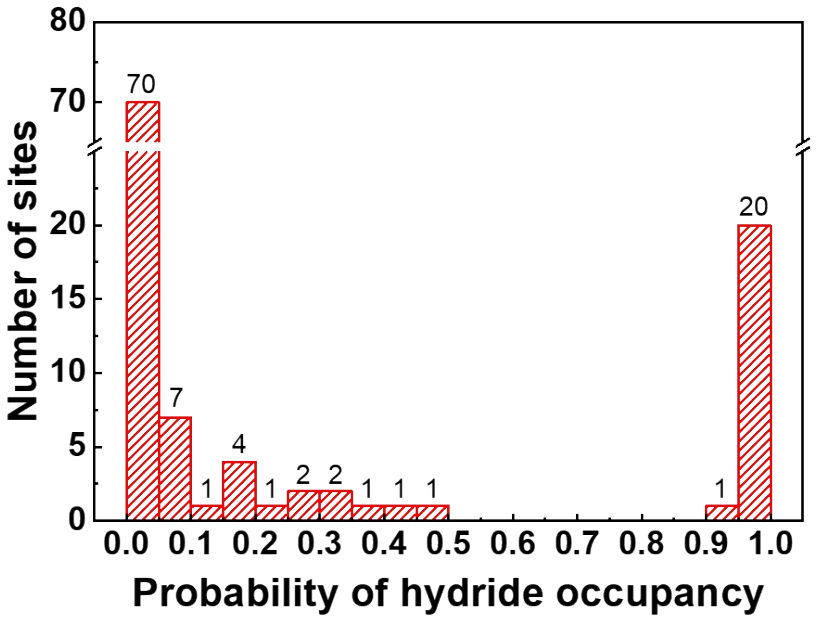

Fig. S8 Probability of hydride occupancy in the Cu_{58} NC predicted by our machine learning model. The plot shows very distinctly that there are 21 sites whose hydride occupancies are close to 1. After symmetry consideration, we eliminated one site (being the center of the cluser) from the 21 sites; the remaining 20 hydrides form the most probable configuration. After placing the 20 hydrides according to the most probable configuration into the X-ray structure, we performed DFT geometry optimization of the total structure and found very minimal disturbance to the X-ray structure.

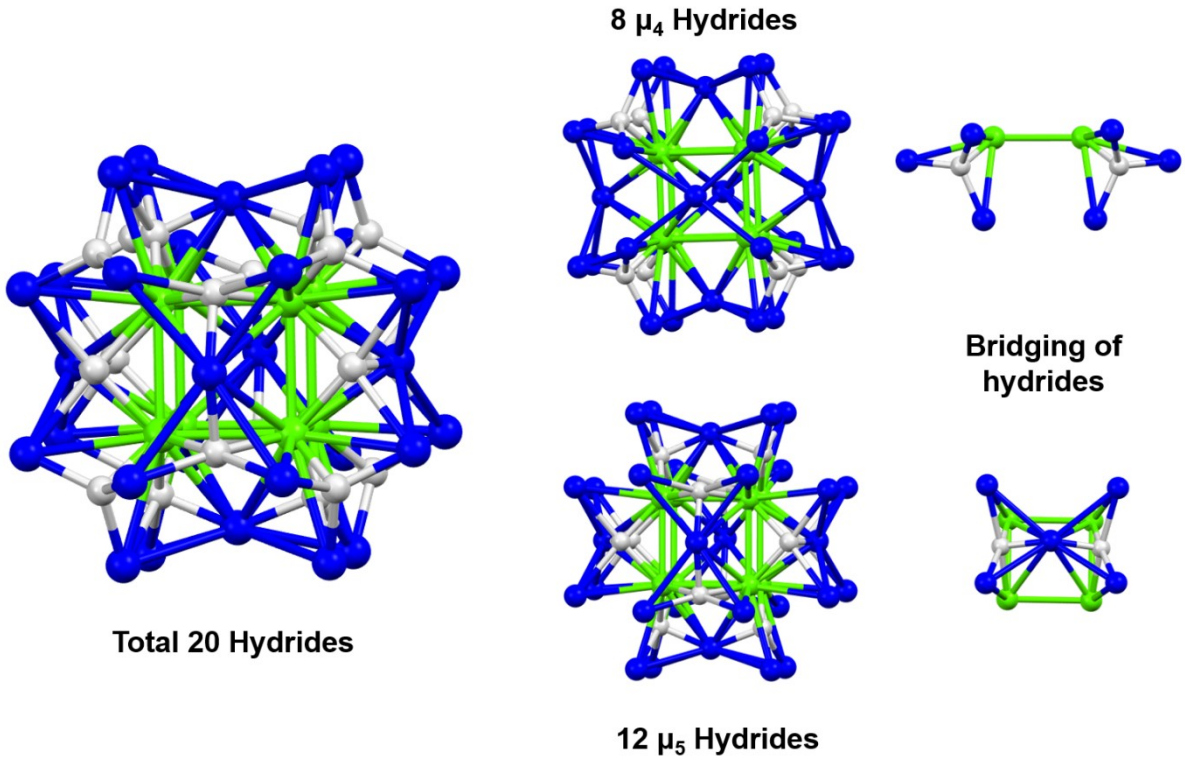

Fig. S9 Position of hydrides inside the Cu58 NC and their bridging mode. Color legend: Cu, light green, blue; H, white.

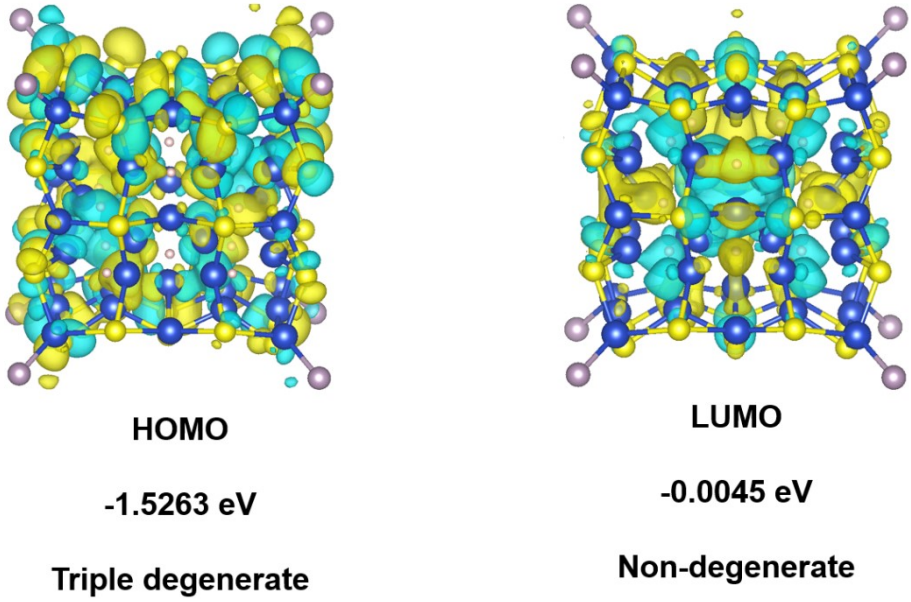

Fig. S10 Orbital arrangements of HOMO and LUMO.

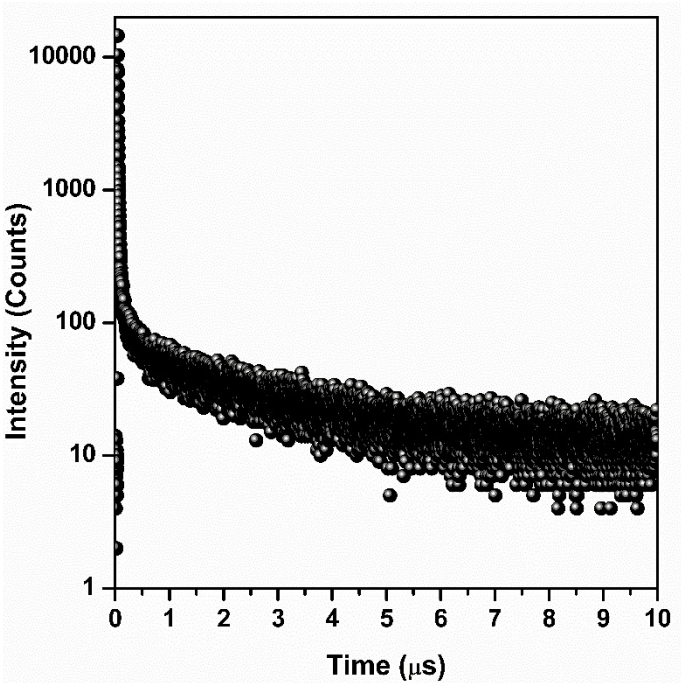

Fig. S11 TCSPC Lifetime of the emission of Cu_{58} NC in $CHCl_3$ solution.

References

S1. G. M. Sheldrick, *Acta Crystallogr., Sect. C: Struct. Chem.* 2015, **71**, 3–8.

S2. Bruker APEX3, v2019.1–0, Bruker AXS Inc., Madison, WI, USA, (2019).

S3. O. V. Dolomanov, L. J. Bourhis, R. J. Gildea, J. A. K. Howard, and H. Puschmann, *J. Appl. Crystallogr*. 2009, **42**, 339–341.

S4. S. Wang, T. Liu, D.-e. Jiang, Locating Hydrides in Ligand-Protected Copper Nanoclusters by Deep Learning. *ACS Appl. Mater. Interfaces* 2021, **13**, 53468–53474.

S5. S. Wang, Z. Wu, S. Dai, et al., Deep Learning Accelerated Determination of Hydride Locations in Metal Nanoclusters. *Angew. Chem., Int. Ed.* 2021, **60**, 12289–12292.

S6. J. P. Perdew, K. Burke, M. Ernzerhof, Generalized Gradient Approximation Made Simple. *Phys. Rev. Lett.* 1996, **77**, 3865.

S7. P E. Blöchl, Projector Augmented-Wave Method. *Phys. Rev. B*, 1994, **50**, 17953.